IEEE Access
Multidisciplinary ⋮ Rapid Review ⋮ Open Access Journal

Received January 27, 2021, accepted February 12, 2021, date of publication February 18, 2021, date of current version March 5, 2021.

*Digital Object Identifier 10.1109/ACCESS.2021.3060080*

# Multi-Anticipative Average Flux Effect in the Lattice Hydrodynamic Model

**HUA KUANG[1], FENGLAN YANG[1], MEITING WANG[1], GUANGHAN PENG[1], AND XINGLI LI[2]**
[1]College of Physical Science and Technology, Guangxi Normal University, Guilin 541004, China
[2]School of Applied Science, Taiyuan University of Science and Technology, Taiyuan 030024, China

Corresponding authors: Hua Kuang (khphy@gxnu.edu.cn) and Xingli Li (lixingli80@163.com)

This work was supported in part by the National Natural Science Foundation of China under Grant 11762004, Grant 11947413, and Grant 61963008; in part by the Natural Science Foundation of Shanxi Province, China, under Grant 201901D111255; and in part by the Innovation Project of Guangxi Graduate Education, China.

**ABSTRACT** The modeling of traffic dynamics under intelligent transportation system (for short, ITS) is an important and interesting topic in traffic flow theory. In this paper, a novel lattice hydrodynamic model is presented to describe dynamic features of traffic flow with consideration of multi-anticipative average flux effect under ITS environment. The corresponding stability condition is obtained by using the linear stability analysis theory. The analytical results show that the stable region can be significantly widened on the phase diagram when the multi-anticipative average flux effect is considered, and the anticipating average flux information of more sites ahead can further lead to the stability of traffic flow. The mKdV equation near the critical point during the nonlinear analysis is derived to describe the evolution properties of traffic density waves by applying the reductive perturbation method. Numerical simulation results are consistent with the theoretical results, which further confirm that the traffic jam can be effectively alleviated by taking into account multi-anticipative average flux effect in the traffic system.

**INDEX TERMS** Traffic flow, lattice hydrodynamic model, multi-anticipative average flux.

## I. INTRODUCTION

Over the past few decades, more and more automobiles on roads make traffic jams become one of the most serious problems, which have aroused wide concern from many scientists and scholars due to its complex mechanism [1]. A considerable variety of traffic flow models have been constructed and developed in order to reveal the properties of traffic jams. Generally, these models can be categorized into the microscopic models (e.g., cellular automaton models [2]–[4] and car-following models [5]–[14]) and the macroscopic models (e.g., hydrodynamic models [15]–[18], lattice hydrodynamic models [19]–[29]). The macroscopic models describe traffic flow similar to the motion of liquid or gas, while the microscopic models represent individual vehicle's movement.

As the simple form of hydrodynamic models, lattice hydrodynamic models have been widely applied to describe the dynamical phase transitions and the stability of traffic flow due to the convenience of calculation and analysis. In 1998, Nagatani [20] firstly presented a simple lattice hydrodynamic model of one-lane freeway, which is very favorable to reflect traffic jamming transition and dynamical evolution of traffic jams by analyzing the mKdV equation. Subsequently, a lot of extended lattice models considering various kinds of traffic factors such as backward-looking or forward-looking effects [21]–[23], and the density or flux difference effects [24]–[26], were presented. Moreover, the optimal control method is introduced to analyze various traffic phenomena [27]–[29], and lane changing is considered to develop the two-lane lattice hydrodynamic models [30]–[33].

With the rapid development of information and communication technologies, the real-time traffic information service system is gradually becoming widely available. In order to improve the transportation efficiency and decrease traffic jams evidently, traffic control system has been applied as an important part of ITS. Drivers can easily acquire more and accurate traffic information about other vehicles in their surrounding and the current road condition, such as the average velocity (or headway) of preceding vehicle group and the average flux of road ahead on a segment. Based on that information, drivers can predict the future state of traffic flow ahead and adjust their driving behavior promptly so as to

The associate editor coordinating the review of this manuscript and approving it for publication was Chi-Hua Chen.

avoid the appearance of a traffic jam. Several lattice traffic models have been established to explore traffic dynamical characteristics in ITS environment. Ge *et al.* [34] proposed a cooperative driving lattice model with consideration of an arbitrary number of front lattice sites. Wang *et al.* [35] constructed a novel lattice model by taking the multiple density difference effect. Redhu and Gupta [36] presented a multi-phase lattice model by accounting for the effect of multi-forward looking sites on highway. Li *et al.* [37] developed an improved lattice model by considering the multiple optimal current differences' anticipation effect. The above results show that the stability of traffic flow can be enhanced greatly by incorporating the traffic information of more front lattice sites.

Recently, the related works of traffic flow stability and dynamics have been further investigated. Song and Zhu [12] analyzed the stability of the classical car-following system by applying the state feedback control strategy. Klawtanong and Limkumnerd [13] studied the dynamics properties of traffic flow by using the stochastic car-following model with modified optimal velocity on circular road. Based on optimal control theory, Zhao *et al.* [27] proposed a novel two-dimensional vehicular movement model to simulate the characteristics of traffic flow at intersections. Cheng and Wang [28] put forward an extended lattice hydrodynamic model to study the effect of delayed feedback control on a curved road. Qin *et al.* [29] proposed a new feedback control model to consider the memory effect of flux difference.

However, the combined effect of the average flux difference and the mean expected flux field (i.e., multi-anticipative average flux effect) on the formation mechanism of traffic density wave has not been explored in the lattice hydrodynamic models up to now. In fact, these two effects can better reflect the road traffic situation ahead and the driver's expected driving behavior. For instance, if the average flux of road ahead is less than the current flux at the same time, which means that the congested flow may occur on road ahead, the drivers will probably determine the deceleration due to the decrease of the expected average flux; on the contrary, the occurrence of free flow can tell the drivers to accelerate considering the increase of the expected average flux. How do these two coupling factors affect the traffic flow stability? Which one is more important in enhancing the stability of traffic flow and alleviating traffic jam? This is an interesting but still open problem.

Therefore, based on above analysis, different from the previous studies, we explore the combined effect of the average flux difference and the mean expected flux field (i.e., multi-anticipative average flux effect) on the stability of traffic flow and the evolution of traffic jams from a new research perspective. In the following section, a novel mean expected optimal flux field including weighted factor is introduced in the new lattice hydrodynamic model. The linear and nonlinear stability analyses are conducted in Section III and Section IV, respectively. In Section V, numerical simulations are performed to confirm the theoretical analysis results, and the intrinsic mechanism of the corresponding phase transition is discussed in detail. Finally, some conclusions are drawn.

## II. MODEL

Firstly, Nagatani [20] in 1998 developed a simple lattice hydrodynamic model describing the complex mechanism of traffic flow on highway. The model consists of a continuity equation and flow equation as follows:

$$\partial_t \rho + \rho_0 \partial_x (\rho v) = 0 \tag{1}$$

$$\partial_t \rho v = a\rho_0 V(\rho(x+\delta)) - a\rho v \tag{2}$$

where $\rho_0$ is the average density; $a$ is the sensitivity of drivers; $V(\bullet)$ refers to the optimal velocity function which is based on the density; $\delta$ represents the average headway and $\delta = 1/\rho_0$; the local density is expressed as $\rho(x+\delta) = 1/h(x,t)$, where $h(x,h)$ is the headway. The means that the variation of traffic flux $\rho v$ at position $x$ is determined by the difference between the optimal flow $\rho_0 V(\rho(x+\delta))$ at position $x+\delta$ and the actual flow $\rho v$ at position $x$.

Eq. (1) and Eq. (2) can be further written with dimensionless space $x$ (let $x^* = x/\delta$, $x^*$ is indicated as $x$ hereafter) and its lattice version as

$$\partial_t \rho_j + \rho_0 \left(\rho_j v_j - \rho_{j-1} v_{j-1}\right) = 0 \tag{3}$$

$$\partial_t \left(\rho_j v_j\right) = a\rho_0 V\left(\rho_{j+1}(t)\right) - a\rho_j v_j \tag{4}$$

where $j$ indicates the $j$-th site on a one-dimensional lattice; $\rho_j(t)$ and $v_j(t)$ denotes the local density and velocity on site $j$ at time $t$, respectively.

Based on Nagatani's model, Tian *et al.* [25] improved a lattice model by considering the flux difference effect. The model is given as follows:

$$\partial_t \rho_j + \rho_0 \left(\rho_j v_j - \rho_{j-1} v_{j-1}\right) = 0 \tag{5}$$

$$\partial_t \left(\rho_j v_j\right) = a\rho_0 V\left(\rho_{j+1}(t)\right) - a\rho_j v_j + \lambda\left(Q_{j+1} - Q_j\right) \tag{6}$$

where $Q_j = \rho_j v_j$ and $Q_{j+1} = \rho_{j+1} v_{j+1}$ is the flux on site $j$ and site $j+1$, respectively; $\Delta Q_j = Q_{j+1} - Q_j$ denotes the flux difference between the site $j$ and site $j+1$; $\lambda$ is the reaction coefficient of the flux difference.

After that, some extended lattice models [29], [38], [39] were established by considering the anticipation optimal flux difference and the memory effect of flux difference. Recently, Jiang *et al.* [40] proposed an improved lattice model to study on-ramp and off-ramp by introducing the effect of mean-field flow difference. However, these studies have not considered the combined effect of the average flux difference and the mean expected flux field on real traffic situation. These two factors may influence on traffic flow obviously.

In this paper, we construct a new lattice hydrodynamic traffic flow by taking into account multi-anticipative average flux effect. The corresponding differential equations of the model are as follows:

$$\partial_t \rho_j + \rho_0 \left(\rho_j v_j - \rho_{j-1} v_{j-1}\right) = 0 \tag{7}$$

$$\partial_t \left(\rho_j v_j\right) = a(1-p)\rho_0 V\left(\rho_{j+1}(t)\right) + ap Q_{mf} - a\rho_j v_j + \lambda\left(\overline{Q_j} - Q_j\right) \tag{8}$$

where $Q_{mf} = \frac{\rho_0}{n}\sum_{l=1}^{n} V\left(\rho_{j+1+l}\left(t\right)\right)$ is called as the mean expected flux field which reflects the mean expected optimal flux from the front lattice sites of site $j+1$. $n$ denotes the total number of front lattice sites of site $j+1$. $\overline{Q_j} = \frac{1}{n}\sum_{l=1}^{n}\rho_{j+l}v_{j+l}$ and $\Delta\bar{Q}_j = \bar{Q}_j - Q_j$ are the average flux and the average flux difference of front lattices of site $j$, respectively. The parameter $p$ is the weight of the current optimal flux and the mean expected flux field. Here, $p$ should be less than 0.5, because the influence of the current optimal flux $\rho_0 V\left(\rho_{j+1}\left(t\right)\right)$ is greater than the mean expected flux field $V_{mf}$ due to the greater effect of nearest-neighbor interaction. The larger $p$ is, the more prominent of the mean expected flux field effect is. When $p = 0$ and $\lambda = 0$, the new model becomes Nagatani's model [20]; When $p = 0, \lambda \neq 0$ and $n = 1$, the new model is simplified to Tian's model [25].

By eliminating velocity $v$ in Eqs. (7) and (8), we can obtain the following density equation

$$\begin{aligned}&\partial_t^2\rho_j + a\rho_0^2\left(1-p\right)\left(V\left(\rho_{j+1}\right) - V\left(\rho_j\right)\right)\\&\quad + a\rho_0^2\frac{p}{n}\left(V\left(\rho_{j+n+1}\right) - V\left(\rho_{j+1}\right)\right)\\&\quad + a\partial_t\rho_j - \lambda\left(\frac{1}{n}\sum_{l=1}^{n}\partial_t\rho_{j+l} - \partial_t\rho_j\right) = 0\end{aligned} \tag{9}$$

Here, we use the optimal velocity function in Ref. [41] as follows:

$$V\left(\rho_j\right) = \frac{v_{\max}}{2}\left[\tanh\left(\frac{2}{\rho_0} - \frac{\rho_j}{\rho_0^2} - \frac{1}{\rho_c}\right) + \tanh\left(\frac{1}{\rho_c}\right)\right] \tag{10}$$

where $v_{\max}$ and $\rho_c$ denote the maximum velocity and the safety critical density, respectively. Note that Eq. (10) is a monotonically decreasing function, and it has a turning point and an upper bound at $\rho_j = \rho_c$ when $\rho_0 = \rho_c$.

## III. LINEAR STABILITY ANALYSIS

In this section, the stability of the new model is derived by adopting linear stability analysis method to study the influence of multi-anticipative average flux effect on jamming transition of traffic flow. Supposed the steady state is a uniform traffic flow with the constant density $\rho_0$, and then the optimal velocity is $V(\rho_0)$. Thus, the steady-state solution of the homogeneous traffic flow can be given as

$$\rho_j\left(t\right) = \rho_0, \quad v_j\left(t\right) = V\left(\rho_0\right) \tag{11}$$

Assume $y_j(t)$ is a small deviation from the steady state density $\rho_j(t)$, then the perturbed solution is

$$\rho_j(t) = \rho_0 + y_j(t) \tag{12}$$

Substituting Eqs. (11) and (12) into Eq. (9), we get the linearized equation as

$$\begin{aligned}&\partial_t^2 y_j + a\rho_0^2 V'\left(1-p\right)\left(y_{j+1} - y_j\right) + a\rho_0^2\frac{p}{n}\left(y_{j+n+1} - y_{j+1}\right)\\&\quad + a\partial_t y_j - \lambda\left(\frac{1}{n}\sum_{l=1}^{n}\partial_t y_{j+l} - \partial_t y_j\right) = 0\end{aligned} \tag{13}$$

where $V' = \left.\frac{\mathrm{d}V(\rho_j)}{\mathrm{d}\rho_j}\right|_{\rho_j=\rho_0}$.

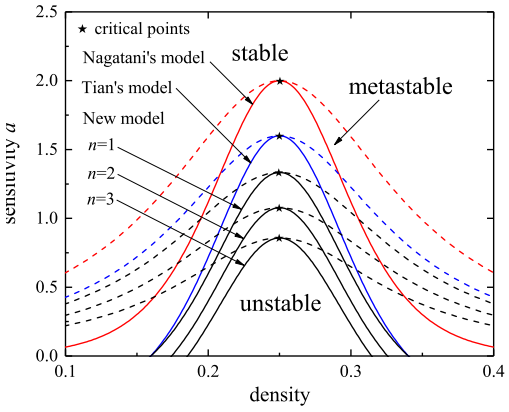


**FIGURE 1.** Phase diagram in the density-sensitivity space for different models.

By further expanding $y_j\left(t\right) = \exp\left(ikj + zt\right)$, we can get equation as follows:

$$\begin{aligned}&z^2 + z\left(a+\lambda\right) + a\rho_0^2 V'\left(1-p\right)\left(e^{ik} - 1\right)\\&\quad + a\rho_0^2 V'\frac{p}{n}\left(e^{ik(n+1)} - e^{ik}\right) - \frac{\lambda z}{n}\sum_{l=1}^{n} e^{ikl} = 0\end{aligned} \tag{14}$$

Inserting $z = ikz_1 + (ik)^2 z_2 + \cdots$ into Eq. (14), the first-order and second-order terms of $ik$ can be derived as:

$$z_1 = -\rho_0^2 V' \tag{15}$$

$$\begin{aligned}z_2 = &-\frac{1}{2}\left(1 + p + pn\right)\rho_0^2 V'\\&+ \frac{1}{2a}\left[\left(1+n\right)\lambda z_1 - 2z_1^2\right]\end{aligned} \tag{16}$$

The uniform steady-state flow is unstable if $z_2 < 0$, while the uniform traffic flow will become stable when $z_2 > 0$. Consequently, the neutral stable criteria for this steady state can be given

$$a = \frac{-2\rho_0^2 V' - \lambda\left(1+n\right)}{1 + p + np} \tag{17}$$

And then, the homogeneous traffic flow will be stable under the following condition:

$$a > \frac{-2\rho_0^2 V' - \lambda\left(1+n\right)}{1 + p + np} \tag{18}$$

As $p = 0, \lambda = 0$, the stable condition is consistent with that of Nagatani's model [20]. As $p = 0, \lambda \neq 0$ and $n = 1$, the stable condition is the same that of Tian's model [25].

Figure 1 gives that the neutral stability curves and the coexisting curves in the density-sensitivity space for different models under different $n$ as $\lambda = 0.2$ and $p = 0.1$. The red, blue and black solid (dotted) lines indicate the neutral stability (the coexisting) curves of the Nagatani's model, Tian's model and new model, respectively. And the asterisks (see the apex of each curve) denote the critical point $(\rho_c, a_c)$. In Fig. 1, we can see clearly that the phase diagram can be divided into three regions: stable, metastable and unstable regions. In the stable region (i.e., the region above the coexistence curve),

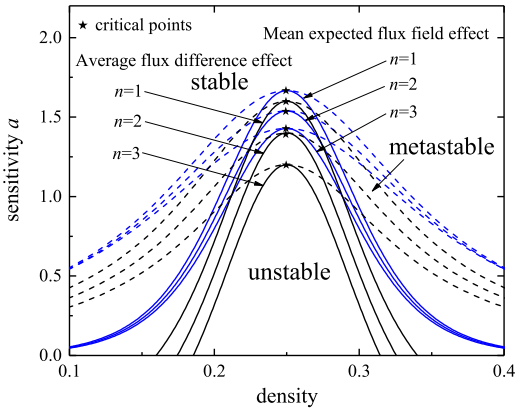


**FIGURE 2. The comparison of phase diagram in the density-sensitivity space between the mean expected flux field effect (i.e., $p \neq 0$, $\lambda = 0$) and the average flux difference effect (i.e., $p = 0$, $\lambda \neq 0$).**

traffic jams will not occur. However, in the metastable region (i.e., the region between the neutral stability and the coexisting curves) and unstable region (i.e., the region below the neutral stability curve), a small disturbance in this unstable traffic flow can lead to the emergence of traffic density waves eventually. Through comparing with Nagatani's model (i.e., $p = 0$, $\lambda = 0$) and Tian's model (i.e., $p = 0$, $\lambda \neq 0$ and $n = 1$), we can observe that the stable region is the largest in the new model (i.e., $n = 1, 2, 3$), which means that the new model is more effective to suppress traffic jams. Furthermore, it can be found that with the increase of the value of $n$, the apex of these curves $(\rho_c, a_c)$ and the neutral stability curves decline gradually, which indicates that the traffic flow will become more stable, and traffic jam will be effectively alleviated if the average flux information of more sites ahead is considered by driver under ITS environment.

In order to compare the contribution of these two effects on the stability of traffic flow, Fig. 2 shows the comparison of phase diagram in the density-sensitivity space between the mean expected flux field effect (i.e., $p \neq 0$, $\lambda = 0$) and the average flux difference effect (i.e., $p = 0$, $\lambda \neq 0$). From Fig.2, we can obviously see that under the same parameter $n$, the neutral and coexisting curves of the average flux difference effect are lower than those of the mean expected flux field effect, which indicates the average flux difference effect plays a more important role than the mean expected flux field effect in enhancing the stability of traffic flow.

## IV. NONLINEAR ANALYSIS

To further investigate the influence of multi-anticipative average flux on the evolution properties of traffic jam, a nonlinear analysis of the new model is further conducted by using the reductive perturbation method for Eq. (9) to explore the system behavior around the critical point $(\rho_c, a_c)$. We define the slow variables $X$ and $T$ for a small positive scaling parameter $\varepsilon(0 < \varepsilon \leq 1)$ are defined as follows [20]:

$$X = \varepsilon (j + bt), \quad T = \varepsilon^3 t \tag{19}$$

where $b$ is a constant to be determined. Let the density $\rho_j$ satisfy the following condition:

$$\rho_j = \rho_c + \varepsilon R(X, T) \tag{20}$$

By expanding each term in Eq. (9) to the fifth order of $\varepsilon$ using of Eqs. (19) and (20), we can obtain

$$\partial_t \rho_j = \varepsilon^2 b \partial_X R + \varepsilon^4 \partial_T R \tag{21}$$

$$\begin{aligned}\partial_t \rho_{j+l} = {} & \varepsilon^2 b \partial_X R + \varepsilon^3 b l \partial_X^2 R \\ & + \varepsilon^4 \left( \frac{1}{2} b l^2 \partial_X^3 R + \partial_T R \right) \\ & + \varepsilon^5 \left( \frac{1}{6} b l^3 \partial_X^4 R + l \partial_X \partial_T R \right)\end{aligned} \tag{22}$$

$$\partial_t^2 \rho_j = \varepsilon^3 b^2 \partial_X^2 R + \varepsilon^5 2 b \partial_X \partial_T R \tag{23}$$

$$\begin{aligned}\rho_{j+1} = {} & \rho_c + \varepsilon R + \varepsilon^2 \partial_X R + \frac{1}{2} \varepsilon^3 \partial_X^2 R \\ & + \frac{1}{6} \varepsilon^4 \partial_X^3 R + \frac{1}{24} \varepsilon^5 \partial_X^4 R\end{aligned} \tag{24}$$

$$\begin{aligned}\rho_{j+n+1} = {} & \rho_c + \varepsilon R + \varepsilon^2 (1+n) \partial_X R \\ & + \frac{1}{2} (1+n)^2 \varepsilon^3 \partial_X^2 R \\ & + \frac{1}{6} (1+n)^3 \varepsilon^4 \partial_X^3 R + \frac{1}{24} (1+n)^4 \varepsilon^5 \partial_X^4 R\end{aligned} \tag{25}$$

$$V(\rho_j) = V + \varepsilon V' R + \frac{1}{6} \varepsilon^3 V''' R^3 \tag{26}$$

$$\begin{aligned}V(\rho_{j+1}) = {} & V + \varepsilon R V' + \varepsilon^2 V' \partial_X R \\ & + \varepsilon^3 \left( \frac{1}{6} R^3 V''' + \frac{1}{2} V' \partial_X^2 R \right) \\ & + \varepsilon^4 \left( \frac{1}{2} R^2 V''' \partial_X R + \frac{1}{6} V' \partial_X^3 R \right) \\ & + \varepsilon^5 \begin{pmatrix} \frac{1}{2} R V''' (\partial_X R)^2 \\ + \frac{1}{4} R^2 V''' \partial_X^2 R + \frac{1}{24} V' \partial_X^4 R \end{pmatrix}\end{aligned} \tag{27}$$

$$\begin{aligned}V(\rho_{j+n+1}) = {} & V + \varepsilon R V' + (1+n) \varepsilon^2 V' \partial_X R \\ & + \varepsilon^3 \left[ \frac{1}{6} R^3 V''' + \frac{1}{2} (1+n)^2 V' \partial_X^2 R \right] \\ & + \varepsilon^4 \left[ \frac{1}{2} (1+n) R^2 V''' \partial_X R + \frac{1}{6} (1+n)^3 V' \partial_X^3 R \right] \\ & + \varepsilon^5 \begin{bmatrix} \frac{1}{2} (1+n)^2 R V''' (\partial_X R)^2 \\ + \frac{1}{4} (1+n)^2 R^2 V''' \partial_X^2 R + \frac{1}{24} (1+n)^4 V' \partial_X^4 R \end{bmatrix}\end{aligned} \tag{28}$$

where $V' = \left. \frac{\mathrm{d}V(\rho_j)}{\mathrm{d}\rho_j} \right|_{\rho_j = \rho_c}$, $V''' = \left. \frac{\mathrm{d}^3 V(\rho_j)}{\mathrm{d}^3 \rho_j} \right|_{\rho_j = \rho_c}$.

By substituting Eqs. (21)-(28) into Eq. (9) and making the Taylor series expansion to the fifth-order of $\varepsilon$, we obtain the following nonlinear partial differential

equation:

$$\begin{aligned}
&\varepsilon^2\left(b+\rho_c^2V'\right)\partial_X R\\
&+\varepsilon^3\left\{\frac{b\left(2b-n\lambda-\lambda\right)}{2a}+\frac{\left(np+p+1\right)\rho_c^2V'}{2}\right\}\partial_X^2R\\
&+\varepsilon^4\left\{\begin{array}{c}\partial_T R+\dfrac{\rho_c^2V'''}{6}\partial_X R^3-\dfrac{b\lambda\left(2n^2+3n+1\right)}{12a}\partial_X^3R\\ +\dfrac{\left(n^2p+3np+2p+1\right)\rho_c^2V'}{6}\partial_X^3R\end{array}\right\}\\
&+\varepsilon^5\left\{\begin{array}{c}\dfrac{4b-\lambda\left(n+1\right)}{2a}\partial_X\partial_T R-\dfrac{bn\lambda\left(n+1\right)^2}{24a}\partial_X^4R\\ +\dfrac{\left(n^3p+4n^2p+6np+3p+1\right)\rho_c^2V'}{24}\partial_X^4R\\ +\dfrac{\left(np+p+1\right)\rho_c^2V'''}{12}\partial_X^2R^3\end{array}\right\}=0
\end{aligned}\tag{29}$$

Near the critical point $(\rho_c, a_c)$, let $a_c = a\left(1+\varepsilon^2\right)$. By taking $b=-\rho_c^2V'$ and eliminating the second-order and third-order terms of $\varepsilon$ in Eq. (29), one can get the following simplified equation:

$$\begin{aligned}
&\varepsilon^4\left(\partial_T R-g_1\partial_X^3R+g_2\partial_X R^3\right)\\
&\qquad+\varepsilon^5\left(g_3\partial_X^2R+g_4\partial_X^4R+g_5\partial_X^2R^3\right)=0
\end{aligned}\tag{30}$$

where

$$g_1=-\frac{1}{6}\rho_c^2V'-\frac{p\left(n+1\right)\left(n+p\right)}{6}\rho_c^2V'-\frac{\lambda\left(2n^2+3n+1\right)}{12a_c}\rho_c^2V'\tag{31}$$

$$g_2=\frac{1}{6}\rho_c^2V'''\tag{32}$$

$$g_3=-\frac{1}{2}\left(np+p+1\right)\rho_c^2V'\tag{33}$$

$$\begin{aligned}
g_4=&\frac{\left[1+p\left(n+1\right)\left(n+2\right)\right]\rho_c^4V'^2}{3a_c}\\
&+\frac{\lambda\left(2n^2+3n+1\right)\rho_c^4V'^2}{6a_c^2}\\
&+\frac{\lambda^2\left(1+n\right)^2\left(1+2n\right)\rho_c^2V'}{24a_c^2}\\
&+\frac{\lambda\left(n+1\right)\left[n^2\left(2p+1\right)+n\left(6p+1\right)+4p+2\right]\rho_c^2V'}{24a_c}\\
&+\frac{\left[1+p\left(n^3+4n^2+6n+3\right)\right]\rho_c^2V'}{24}
\end{aligned}\tag{34}$$

$$g_5=\frac{a_c\left(np+p+1\right)+\lambda\left(n+1\right)+4\rho_c^2V'}{12a_c}\rho_c^2V'''\tag{35}$$

To get the regularized mKdV equation from Eq. (30), we perform the following transformations:

$$T'=g_1T,\ R=\sqrt{\frac{g_1}{g_2}}R'\tag{36}$$

Then, Eq. (30) can be transformed to the standard mKdV equation with correction term $O(\varepsilon)$ as follows:

$$\partial_{T'}R'-\partial_X^3R'+\partial_XR'^3+\varepsilon M\left[R'\right]=0\tag{37}$$

where $M\left[R'\right]=\frac{1}{g_1}\left[g_3\partial_X^2R'+g_4\partial_X^4R'+\frac{g_1g_5}{g_2}\partial_X^2R'^3\right]$

After ignoring the $O(\varepsilon)$ terms in Eq. (37), the kink-antikink solution of the mKdV equation can be derived as follows:

$$R_0'\left(X,T'\right)=\sqrt{c}\tanh[\sqrt{\frac{c}{2}}\left(X-cT'\right)]\tag{38}$$

where $c$ is the propagation velocity of the kink-antikink solution and its value is decided by solving the following solvability condition [6]:

$$\left(R_0',M\left[R_0'\right]\right)\equiv\int_{-\infty}^{+\infty}\mathrm{d}X'R_0'M\left[R_0'\right]=0\tag{39}$$

where $M\left[R_0'\right]=M\left[R_0\right]$.

Thus, we can obtain the following general solution of $c$:

$$c=\frac{5g_2g_3}{2g_2g_4-3g_1g_5}\tag{40}$$

Then, we can derive the solution of mKdV equation as

$$\begin{aligned}
\Delta\rho_j\left(t\right)=\rho_c+\sqrt{\frac{g_1c}{g_2}\left(\frac{a_c}{a}-1\right)}\tanh\sqrt{\frac{c}{2}\left(\frac{a_c}{a}-1\right)}\\
\times\left[j+\left(1-cg_1\left(\frac{a_c}{a}-1\right)t\right)\right]
\end{aligned}\tag{41}$$

And the amplitude $A$ of the kink-antikink solution is obtained by

$$A=\sqrt{\frac{g_1c}{g_2}\left(\frac{a_c}{a}-1\right)}\tag{42}$$

The kink-antikink solution represents the coexisting phase of the low-density freely moving phase and the high-density congested phase. They can be expressed by $\rho_j=\rho_c-A$ and $\rho_j=\rho_c+A$ (see the coexisting curves, i.e., the dotted lines in Fig.1 and Fig.2) in the density-sensitivity space, respectively.

## V. NUMERICAL SIMULATION AND RESULTS ANALYSIS

For the convenience of simulation, we rewrite Eq. (9) into the following difference form:

$$\begin{aligned}
&\rho_j\left(t+2\tau\right)-\rho_j\left(t+\tau\right)\\
&\quad+\tau\rho_0^2\left\{\begin{array}{c}\left(1-p\right)\left[V\left(\rho_{j+1}\left(t\right)\right)-V\left(\rho_j\left(t\right)\right)\right]\\ +\dfrac{p}{n}\left[V\left(\rho_{j+n+1}\left(t\right)\right)-V\left(\rho_{j+1}\left(t\right)\right)\right]\end{array}\right\}\\
&\quad+\lambda\tau\left[\rho_j\left(t+\tau\right)-\rho_j\left(t\right)\right]\\
&\quad-\frac{\tau\lambda}{n}\sum_{l=1}^{n}\left[\rho_{j+l}\left(t+\tau\right)-\rho_{j+l}\left(t\right)\right]=0
\end{aligned}\tag{43}$$

To verify the theoretical results and reveal the impact of multi-anticipative average flux effect on traffic flow, we choose the fourth-order Runge-Kutta method to simulate

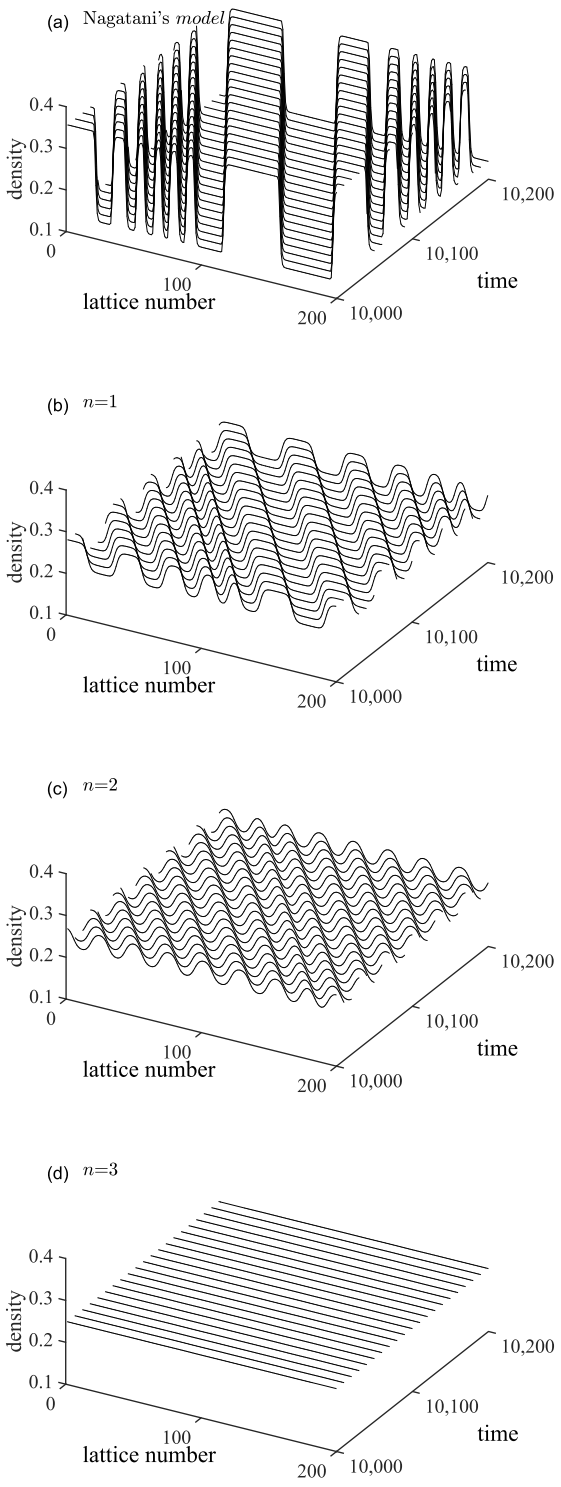


**FIGURE 3.** Space-time evolution of the density after t = 10000 time steps, where $a = 0.98$.

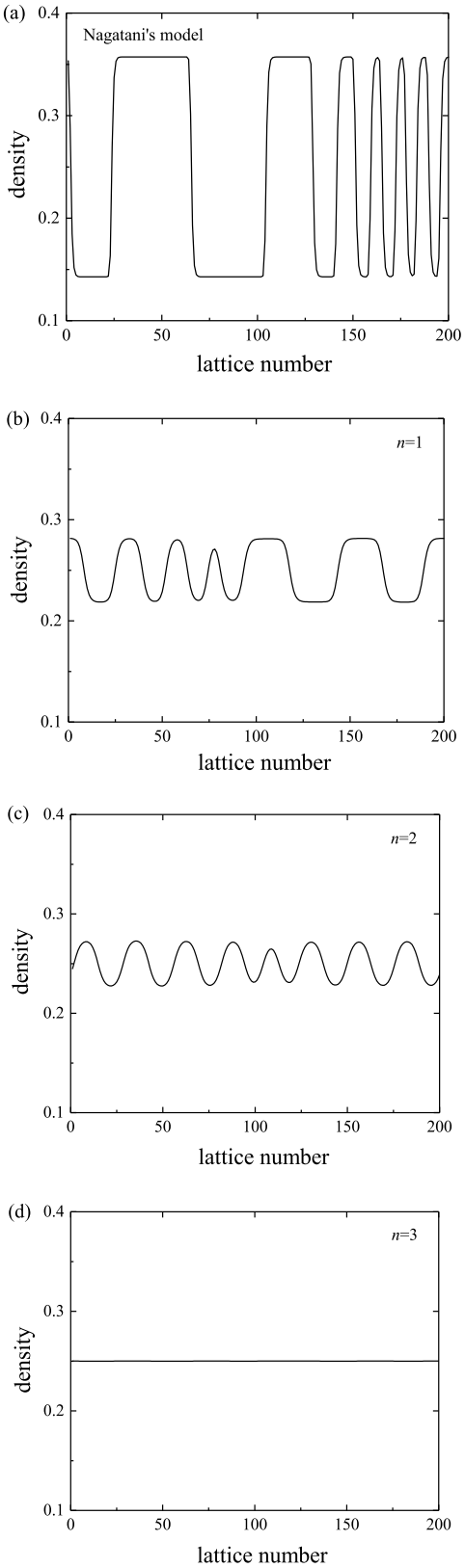


**FIGURE 4.** Density profiles of density waves at $t = 10200$ corresponding to patterns in Fig. 3, respectively.

the new model described by Eq. (43). The periodic boundary is used by choosing the following initial conditions:

$$\rho_j(0) = \rho_0 = 0.25,$$
$$\rho_j(1) = 0.25 \ (j \neq 100, 101) \tag{44}$$
$$\rho_j(1) = 0.25 - 0.01 \ (j = 100) \tag{45}$$
$$\rho_j(1) = 0.25 + 0.01 \ (j = 101) \tag{46}$$

In the simulation, the total lattice is $N = 200$, $v_{\max} = 2$, $p = 0.1$, $\lambda = 0.2$ and $a = 0.98$.

Figure 3 depicts the simulation results of the space-time evolution of the density after $t = 10000$ time steps. Fig. 3(a) exhibits the results of Nagatani's model (i.e., $p = 0$ and $\lambda = 0$). Figs. 3(b)-(d) display the density evolution of the new model corresponding to the three cases of n = 1, 2 and 3, with $p = 0.1$ and $\lambda = 0.2$, respectively. From Fig. 3(a)-(c), one can see clearly that a small stochastic disturbance will make the initial stable traffic flow evolve into traffic density waves propagating backwards, because the stability criterion of Eq. (18) has not been met as $a = 0.98$. The propagating behaviour of the congested traffic waves can be characterized by the kink-antikink solution of the mKdV equation corresponding to the nonlinear analytical results in Section IV. Meanwhile, one can find that the traffic stability will become better and better with increasing n, especially, the initial disturbed traffic flow will recover to its stable state and the density wave will disappear after a long time as shown in Fig. 3 (d), which means that the multi-anticipative average flux effect can strength the stability of traffic flow obviously, and suppress the traffic jams effectively.

Figure 4 displays the density profile obtained at $t = 10200$ corresponding to Fig. 3. It can be observed obviously that the amplitude fluctuation of Nagatani's model is much larger than those of the new model, which indicates that the traffic jams appear more easily and are difficult to evanish when the multi-anticipative average flux effect is neglected. Additionally, as the value of $n$ increases, the fluctuation of the density decreases gradually until it disappears when $n = 3$. All these results show that taking into account the multi-anticipative average flux effect can improve the traffic stability effectively, which further verifies the above linear and nonlinear analytical results.

## VI. CONCLUSION

In this paper, we established a new lattice hydrodynamic model by considering the multi-anticipative average flux effect under ITS environment. The stability condition and mKdV equation near the critical point are obtained by using the linear stability analysis and nonlinear analysis theory, respectively. The phase diagram comparison and analysis show that the new model has the largest stable region among three models. Moreover, stabilizing traffic flow is more influenced by the average flux difference effect than the mean expected flux field effect. The simulation results also demonstrate that considering multi-anticipative average flux effect and increasing the number of the sizes ahead can effectively improve the stability of traffic flow, which are in good accordance with the theoretical findings. Hence, it is reasonable to consider the multi-anticipative average flux effect to alleviate traffic congestion in traffic flow modeling.

In the future, some research based on other models and the corresponding comparison will be done. Besides, we will further explore the two-lane lattice model by incorporating lane-changing behaviors and other important aspects (e.g., the driver's attributions).

## REFERENCES


[1] T. Nagatani, "The physics of traffic jams," *Rep. Prog. Phys.*, vol. 65, no. 9, pp. 1331–1386, Aug. 2002.

[2] S. Maerivoet and B. De Moor, "Cellular automata models of road traffic," *Phys. Rep.*, vol. 419, no. 1, pp. 1–64, Nov. 2005.

[3] N. Cui, B. Chen, K. Zhang, Y. Zhang, X. Liu, and J. Zhou, "Effects of route guidance strategies on traffic emissions in intelligent transportation systems," *Phys. A, Stat. Mech. Appl.*, vol. 513, pp. 32–44, Jan. 2019.

[4] Y. J. Zhou, H. B. Zhu, M. M. Guo, and J. L. Zhou, "Impact of CACC vehicles' cooperative driving strategy on mixed four-lane highway traffic flow," *Phys. A, Stat. Mech. Appl.*, vol. 540, Feb. 2020, Art. no. 122721.

[5] M. Bando, K. Hasebe, A. Nakayama, A. Shibata, and Y. Sugiyama, "Dynamical model of traffic congestion and numerical simulation," *Phys. Rev. E, Stat. Phys. Plasmas Fluids Relat. Interdiscip. Top.*, vol. 51, no. 2, pp. 1035–1042, Feb. 1995.

[6] T. Nagatani, "Thermodynamic theory for the jamming transition in traffic flow," *Phys. Rev. E, Stat. Phys. Plasmas Fluids Relat. Interdiscip. Top.*, vol. 58, no. 4, pp. 4271–4276, Oct. 1998.

[7] R. Jiang, Q. Wu, and Z. Zhu, "Full velocity difference model for a car-following theory," *Phys. Rev. E, Stat. Phys. Plasmas Fluids Relat. Interdiscip. Top.*, vol. 64, no. 1, Jun. 2001, Art. no. 017101.

[8] Y. Sun, H. Ge, and R. Cheng, "An extended car-following model under V2 V communication environment and its delayed-feedback control," *Phys. A, Stat. Mech. Appl.*, vol. 508, pp. 349–358, Oct. 2018.

[9] Z. Wen-Xing and Z. Li-Dong, "A new car-following model for autonomous vehicles flow with mean expected velocity field," *Phys. A, Stat. Mech. Appl.*, vol. 492, pp. 2154–2165, Feb. 2018.

[10] M. Zhao, S.-H. Wang, D. Sun, and X.-J. Wang, "A car-following model considering preceding Vehicle's lane-changing process," *IEEE Access*, vol. 7, pp. 89913–89923, 2019.

[11] H. Kuang, M.-T. Wang, F.-H. Lu, K.-Z. Bai, and X.-L. Li, "An extended car-following model considering multi-anticipative average velocity effect under V2 V environment," *Phys. A, Stat. Mech. Appl.*, vol. 527, Aug. 2019, Art. no. 121268.

[12] T. Song and W.-X. Zhu, "Study on state feedback control strategy for car-following system," *Phys. A, Stat. Mech. Appl.*, vol. 558, Nov. 2020, Art. no. 124938.

[13] M. Klawtanong and S. Limkumnerd, "Dissipation of traffic congestion using autonomous-based car-following model with modified optimal velocity," *Phys. A, Stat. Mech. Appl.*, vol. 542, Mar. 2020, Art. no. 123412.

[14] J. Zhang, B. Wang, S. Li, T. Sun, and T. Wang, "Modeling and application analysis of car-following model with predictive headway variation," *Phys. A, Stat. Mech. Appl.*, vol. 540, Feb. 2020, Art. no. 123171.

[15] P. Zhang, R.-X. Liu, and S. C. Wong, "High-resolution numerical approximation of traffic flow problems with variable lanes and free-flow velocities," *Phys. Rev. E, Stat. Phys. Plasmas Fluids Relat. Interdiscip. Top.*, vol. 71, no. 5, May 2005, Art. no. 056704.

[16] H. Ou and T.-Q. Tang, "Impacts of moving bottlenecks on traffic flow," *Phys. A, Stat. Mech. Appl.*, vol. 500, pp. 131–138, Jun. 2018.

[17] L. Yu, "A new continuum traffic flow model with two delays," *Phys. A, Stat. Mech. Appl.*, vol. 545, May 2020, Art. no. 123757.

[18] Z. Wang, H. Ge, and R. Cheng, "An extended macro model accounting for the driver's timid and aggressive attributions and bounded rationality," *Phys. A, Stat. Mech. Appl.*, vol. 540, Feb. 2020, Art. no. 122988.

[19] Z.-M. Zhou, M. Zhao, D. Chen, Y.-C. Zhang, and D.-H. Sun, "An extended mean-field lattice hydrodynamic model with consideration of the average effect of multi-lattice interaction," *IEEE Access*, vol. 7, pp. 168798–168804, 2019.

[20] T. Nagatani, "Modified KdV equation for jamming transition in the continuum models of traffic," *Phys. A, Stat. Mech. Appl.*, vol. 261, nos. 3–4, pp. 599–607, Dec. 1998.

[21] C. T. Jiang, R. J. Cheng, and H. X. Ge, "An improved lattice hydrodynamic model considering the 'backward looking' effect traffic interruption probability," *Nonlinear Dyn.*, vol. 91, pp. 777–784, Nov. 2018.

[22] Q. Y. Wang and H. X. Ge, "An improved lattice hydrodynamic model accounting for the effect of 'backward looking' flow integral," *Phys. A, Stat. Mech. Appl.*, vol. 513, pp. 438–446, Jan. 2019.

[23] Y. Wang, H. Ge, and R. Cheng, "An improved lattice hydrodynamic model considering the influence of optimal flux for forward looking sites," *Phys. Lett. A*, vol. 381, no. 41, pp. 3523–3528, Nov. 2017.

[24] C. Jiang, R. Cheng, and H. Ge, "Effects of speed deviation and density difference in traffic lattice hydrodynamic model with interruption," *Phys. A, Stat. Mech. Appl.*, vol. 506, pp. 900–908, Sep. 2018.
[25] T. Jun-Fang, J. Bin, L. Xing-Gang, and G. Zi-You, "Flow difference effect in the lattice hydrodynamic model," *Chin. Phys. B*, vol. 19, no. 4, Apr. 2010, Art. no. 040303.
[26] S. Sharma, "Effect of driver's anticipation in a new two-lane lattice model with the consideration of optimal current difference," *Nonlinear Dyn.*, vol. 81, nos. 1–2, pp. 991–1003, Jul. 2015.
[27] J. Zhao, V. L. Knoop, and M. Wang, "Two-dimensional vehicular movement modelling at intersections based on optimal control," *Transp. Res. B, Methodol.*, vol. 138, pp. 1–22, Aug. 2020.
[28] R. Cheng and Y. Wang, "An extended lattice hydrodynamic model considering the delayed feedback control on a curved road," *Phys. A, Stat. Mech. Appl.*, vol. 513, pp. 510–517, Jan. 2019.
[29] S. Qin, Z. He, and R. Cheng, "An extended lattice hydrodynamic model based on control theory considering the memory effect of flux difference," *Phys. A, Stat. Mech. Appl.*, vol. 509, pp. 809–816, Nov. 2018.
[30] G. Peng, S. Yang, D. Xia, and X. Li, "A novel lattice hydrodynamic model considering the optimal estimation of flux difference effect on two-lane highway," *Phys. A, Stat. Mech. Appl.*, vol. 506, pp. 929–937, Sep. 2018.
[31] G. Peng, H. Kuang, H. Zhao, and L. Qing, "Nonlinear analysis of a new lattice hydrodynamic model with the consideration of honk effect on flux for two-lane highway," *Phys. A, Stat. Mech. Appl.*, vol. 515, pp. 93–101, Feb. 2019.
[32] G. Peng, D. Xia, and S. Yang, "The stability of traffic flow on two lanes incorporating driver's characteristics corresponding to honk effect under V2X environment," *IEEE Access*, vol. 8, pp. 73879–73889, 2020.
[33] J. Zhang, K. Xu, S. Li, and T. Wang, "A new two-lane lattice hydrodynamic model with the introduction of driver's predictive effect," *Phys. A, Stat. Mech. Appl.*, vol. 551, Aug. 2020, Art. no. 124249.
[34] H. X. Ge, S. Q. Dai, Y. Xue, and L. Y. Dong, "Stabilization analysis and modified Korteweg–de vries equation in a cooperative driving system," *Phys. Rev. E, Stat. Phys. Plasmas Fluids Relat. Interdiscip. Top.*, vol. 71, no. 6, Jun. 2005, Art. no. 066119.
[35] T. Wang, Z. Gao, and J. Zhang, "Stabilization effect of multiple density difference in the lattice hydrodynamic model," *Nonlinear Dyn.*, vol. 73, no. 4, pp. 2197–2205, May 2013.
[36] P. Redhu and A. K. Gupta, "Effect of forward looking sites on a multi-phase lattice hydrodynamic model," *Phys. A, Stat. Mech. Appl.*, vol. 445, pp. 150–160, Mar. 2016.
[37] X. Li, K. Fang, and G. Peng, "A new lattice model accounting for multiple optimal current differences' anticipation effect in two-lane system," *Phys. A, Stat. Mech. Appl.*, vol. 486, pp. 814–826, Nov. 2017.
[38] D.-H. Sun, G. Zhang, M. Zhao, S.-L. Cheng, and J.-D. Cao, "Stability analysis of feedforward anticipation optimal flux difference in traffic lattice hydrodynamic theory," *Commun. Nonlinear Sci. Numer. Simul.*, vol. 56, pp. 287–295, Mar. 2018.
[39] Y. Y. Chang, Z. T. He, and R. J. Cheng, "An extended lattice hydrodynamic model considering the driver's sensory memory and delayed-feedback control," *Phys. A, Stat. Mech. Appl.*, vol. 514, pp. 522–532, Jan. 2019.
[40] C. T. Jiang, R. J. Cheng, and H. X. Ge, "Mean-field flow difference model with consideration of on-ramp and off-ramp," *Phys. A, Stat. Mech. Appl.*, vol. 513, pp. 465–476, Jan. 2019.
[41] T. Nagatani, "Jamming transition in a two-dimensional traffic flow model," *Phys. Rev. E, Stat. Phys. Plasmas Fluids Relat. Interdiscip. Top.*, vol. 59, no. 5, pp. 4857–4864, May 1999.

**HUA KUANG** received the B.S. and M.S. degrees in physics from Guangxi Normal University, in 2001 and 2004, respectively, and the Ph.D. degree in fluid mechanics from Shanghai University, in 2011. He is currently a Professor with the College of Physical Science and Technology, Guangxi Normal University. His research interests include traffic flow theory, evacuation dynamics, and intelligent transportation systems.

**FENGLAN YANG** received the B.S. degree in physics from Guangxi Normal University, China, in 2019, where she is currently pursuing the master's degree with the College of Physical Science and Technology. Her research interests include traffic flow modeling and density wave analysis.

**MEITING WANG** received the B.S. degree in physics from Huizhou University, China, in 2017. She is currently pursuing the master's degree with the College of Physical Science and Technology, Guangxi Normal University. Her research interests include traffic flow modeling and nonlinear analysis.

**GUANGHAN PENG** received the Ph.D. degree from Chongqing University, in June 2009. He is currently a Professor with the College of Physical Science and Technology, Guangxi Normal University. His research interests include traffic flow theory, intelligent transportation systems, and traffic control.

**XINGLI LI** received the B.S. and M.S. degrees in physics from Shaanxi Normal University, in 2002 and 2005, respectively, and the Ph.D. degree in fluid mechanics from Shanghai University, in 2008. She is currently a Professor with the School of Applied Science, Taiyuan University of Science and Technology. Her research interests include traffic flow theory, evacuation dynamics, and intelligent transportation systems.